Journal of Sound and Vibration 326 (2009) 768–779

Contents lists available at ScienceDirect

Journal of Sound and Vibration

journal homepage: www.elsevier.com/locate/jsvi

Melnikov's criteria and chaos in systems with fractional order deflection

L. Cveticanin *, M. Zukovic

Faculty of Technical Sciences, 21000 Novi Sad, Trg D. Obradovica 6, Serbia

ARTICLE INFO

Article history:
Received 9 October 2008
Received in revised form
4 May 2009
Accepted 6 May 2009
Handling Editor: M.P. Cartmell
Available online 6 June 2009

ABSTRACT

In this paper a qualitative analysis of the dynamic systems described with the second-order differential equation with fractional order deflection function is considered. The existence of fixed points, closed orbits and the unions of fixed points and the trajectories connecting them is shown. The homoclinic orbit which connects a fixed point with itself and the corresponding stable and unstable manifolds are given in the closed analytical form. Melnikov's procedure for defining the criteria for transversal intersection of the stable and unstable manifolds is extended for the systems with fractional order deflection function. The critical parameter values for chaos are obtained analytically and proved numerically using the Lyapunov exponents. The bifurcation diagrams are plotted for various values of fractional order and the transition to chaos by period doubling is shown. The phase plane diagrams and the Poincare maps for certain fractional orders are obtained. The control of chaos and the transformation to periodic motion is considered.

1. Introduction

In this paper the generalized Duffing type differential equation with fractional order nonlinear term is considered

$$\ddot{x} - x + x|x|^{\alpha-1} = \varepsilon(\gamma \cos \omega t - \delta \dot{x}). \tag{1}$$

The constant $\alpha > 1$ is an integer or a fraction. For $\varepsilon \ll 1$ the coefficients $\varepsilon\gamma$ and $\varepsilon\delta$ are small parameters. The frequency of the periodic function is ω. This investigation represents the extension of previous work [1] and the generalization of [2,3] for the Duffing equation with a strong cubic term ($\alpha = 3$)

$$\ddot{x} - x + x^3 = \varepsilon(\gamma \cos \omega t - \delta \dot{x}). \tag{2}$$

The differential equation (1) has a physical meaning. Namely (1) represents the oscillatory motion of a buckled beam with simply supported or hinged ends for the modal displacement $x(t)$ (see [4–6]). The terms on the right-hand side of Eq. (1) correspond to the small excitation and damping force and the terms on the left-hand side are the inertial and the restitution force, respectively. The exponent α in the fraction order power law depends on the material and bending properties of the beam. There are many materials whose elastic properties are not linear. For example, the elastic properties of the aircraft materials: aluminum, titanium, etc., are of Ramberg–Osgood type [7], where α is a fraction higher than 1. For copper and copper alloys, whose elastic properties are of Ludwick type [8,9], the parameter α is a rational number which is

* Corresponding author.
E-mail address: cveticanin@uns.ac.rs (L. Cveticanin).

0022-460X/$ - see front matter © 2009 Elsevier Ltd. All rights reserved.
doi:10.1016/j.jsv.2009.05.012

determined experimentally. The constitutive models of the wood [10], polymers [11] and composite materials [12] are presented in polynomial form where $\alpha = 3$ and the differential equation of beam's motion is of Duffing type [13] with strong cubic nonlinearity.

The vibrations of the piano hammer are also described with (1). The piano hammer is a wooden beam which is coated with several layers of compressed wool felts. The elastic force in the hammer is nonlinear and the exponent α has the values ranging from 2.2 to 3.5 for hammers taken from pianos and 1.5 to 2.8 for new hammers [14].

In the paper [15] the nonlinear vibrations in the vehicle are considered. The properties of the suspension and the tires are nonlinear. The experimentally obtained value for α is about $\frac{3}{2}$.

A vibration model of open celled polyurethane foam automative seat cushions [16,17] has the form (1). The coefficient α is obtained experimentally and has the value 5.945.

Relation (1) describes the phenomena in electronics too. The nonlinearity of the restitution force has an important role in micro-electromechanical systems like micro-oscillators [18], micro-filters [19], and micro-actuators [20]. The investigations done for the micro-actuators [20] give the optimal values for α to be in the interval 4–7.

As it is seen in the previous examples the coefficient α is higher than 1 and need not be an integer. Eq. (1) is with a fractional order term which involves the well-known Duffing equation with cubic nonlinearity (2) and represents the generalized Duffing equation.

In this paper the criteria of chaos and the control of chaos for the system described with (1) and its dependence on the parameter α are investigated. The criteria of chaos are obtained analytically by generalization of Melnikov's procedure [21] which was developed for the Duffing equation with cubic nonlinearity (2) (see [22,23]) and its modifications (for the Duffing equation with complex function [24], Duffing equation with strong cubic and quintic term [25], a three-well Duffing system [26], etc.). In Section 2, the homoclinic orbit for (1) is given in the exact analytical form and according to Melnikov's theorem [21] the rate of change of the distance between stable and unstable manifolds for small perturbations is calculated. The parameter values producing chaotic behavior of the system are determined. The dependence of the critical parameters value on the value of α is explicitly shown. In Section 3, for certain fractional values, the numerical simulation of (1) is done. The phase plane diagrams and the Poincare maps are plotted. In Section 4, the existence of the chaotic motion is proved by calculating the Lyapunov characteristic exponents. The bifurcation diagrams for these fraction values are also plotted and the critical values for chaotic motion are numerically determined. The analytically and numerically obtained critical values are compared and the accuracy of the analytical procedure is proved. In Section 5, the delayed feedback control, the so-called 'Pyragas method' (see [27–33]), is adopted for the chaos control of the fractional order differential equation (1). Usually, for controlling chaos in the equations of Duffing type the feed-forward (also called non-feedback or open-loop) control (see [34–42]) is applied. The feed-forward control is based on the additional perturbation to the system and, then, on determination of the frequency values of excitation which destroy the chaos ([23,25,26] and [36–40]). Unfortunately, the calculation of the new Melnikov's function for the perturbed system is not an easy task. Very often the parameters for chaos suppression are obtained numerically. At the other side, the 'Pyragas method', due to its simplicity, is widely used for control chaos in lasers [43,44], magneto-elastic systems (see [45,46]), the 'traffic models, pulse-width modulation controlled buck converters, paced excitable oscillators described by FitzHugh–Nagumo model widely used in physiology' [47], in Lorenz system [48], but also in coupled electromechanical systems (see [49,50]). In this paper the method of chaos control by delayed self-controlling feedback developed by Pyragas [27–31] is applied for (1). The theoretical considerations are tested on a few examples. The results obtained after control are compared with those before suppressing chaos.

2. Homoclinic orbits in the unperturbed fractional order system

For the unperturbed system with fractional order displacement, when $\varepsilon = 0$, the differential equation (1) simplifies to

$$\ddot{x} - x + x|x|^{\alpha-1} = 0. \tag{3}$$

The system has two centers at $(x, \dot{x}) = (\pm 1, 0)$ and a hyperbolic saddle at $(0, 0)$. The energy function for (3) is

$$\frac{\dot{x}^2}{2} - \frac{x^2}{2} + \frac{x^2|x|^{\alpha-1}}{\alpha+1} = K, \tag{4}$$

where K is the energy constant dependent on the initial amplitude $x(0) = x_0$, initial velocity $\dot{x}(0) = \dot{x}_0$ and fractional order α

$$K = \frac{\dot{x}_0^2}{2} - \frac{x_0^2}{2} + \frac{x_0^2|x_0|^{\alpha-1}}{\alpha+1}. \tag{5}$$

Dependently on K, the level sets are different. For all of them it is common that they form closed periodic orbits which surround the fixed points $(x, \dot{x}) = (1, 0)$ or $(x, \dot{x}) = (-1, 0)$ or all the three fixed points $(\pm 1, 0)$ and $(0, 0)$. The boundary between these two groups of orbits corresponds to $K = 0$, when

$$\dot{x}_0 = \pm\sqrt{x_0^2\left(1 - \frac{2}{\alpha+1}|x_0|^{\alpha-1}\right)}. \tag{6}$$

The level set

$$\frac{\dot{x}^2}{2}-\frac{x^2}{2}+\frac{x^2|x|^{\alpha-1}}{\alpha+1}=0 \tag{7}$$

is composed of two homoclinic orbits

$$\Gamma_+^0(t)\equiv(x_+^0(t),\dot{x}_+^0(t)), \tag{8}$$

$$\Gamma_-^0(t)\equiv(x_-^0(t),\dot{x}_-^0(t)), \tag{9}$$

which connect the fixed hyperbolic saddle point $(0,0)$ to itself and contain the stable and unstable manifolds. The functions $x_\pm^0(t)$ are the exact solution of (7) for

$$x_0=\pm\left(\frac{\alpha+1}{2}\right)^{1/(\alpha-1)},\quad \dot{x}_0=0, \tag{10}$$

i.e.,

$$\Gamma_+^0(t)=\left(\sqrt[\alpha-1]{\frac{\alpha+1}{2}}\left[\operatorname{sech}\left(\frac{\alpha-1}{2}t\right)\right]^{2/(\alpha-1)},-\sqrt[\alpha-1]{\frac{\alpha+1}{2}}\left[\operatorname{sech}\left(\frac{\alpha-1}{2}t\right)\right]^{2/(\alpha-1)}\tanh\left(\frac{\alpha-1}{2}t\right)\right),$$

$$\Gamma_-^0(t)=-\Gamma_+^0(t), \tag{11}$$

where sech and tanh are the hyperbolic functions. Relations (10) and (11) represent the closed form analytical solution for the homoclinic orbits of (1) for $\varepsilon=0$. The relations are the general form of the homoclinic orbits for (1) and are valid for all values of parameter $\alpha>1$, including not only all integer numbers, but also the whichever fractions.

As the special case, let us determine the homoclinic orbit for the case of cubic nonlinearity. Substituting $\alpha=3$ into (10) and (11) the homoclinic orbits for $x_0=\pm\sqrt{2}$ and $\dot{x}_0=0$ have the form

$$\Gamma_+^0(t)=(\sqrt{2}\operatorname{sech}(t),-\sqrt{2}\operatorname{sech}(t)\tanh(t)),\quad \Gamma_-^0(t)=-\Gamma_+^0(t). \tag{12}$$

Comparing (12) with the results given by Guckenheimer and Holmes [2], it is concluded, that they are the same.

Parameters of the homoclinic orbits: The homoclinic orbits form a closed curve which connects the fixed saddle point $(0,0)$ to itself. The extreme characteristics $x_{\max}$ and $\dot{x}_{\max}$ of the homoclinic orbit are according to (10) and (7): $(\pm((\alpha+1)/2)^{1/(\alpha-1)},0)$ and $(\pm1,\pm\sqrt{(\alpha-1)/(\alpha+1)})$. In Table 1 the extreme value $x_{\max}$ and $\dot{x}_{\max}$ of the homoclinic orbit $\Gamma_+^0(t)$ for various fraction values α is calculated.

Analyzing the extreme values in the homoclinic motion, it is concluded that the maximal values $x_{\max}$ and $\dot{x}_{\max}$ depend on the coefficient of fractional order α: the higher the α, the higher the value of $\dot{x}_{\max}$ and smaller the value of $x_{\max}$. For higher values of α both values tend to 1. For $\alpha\approx1$ the maximal value $\dot{x}_{\max}$ tends to zero.

The time period necessary for going from $x_{\max}$ to $\dot{x}_{\max}$ in $x=1$ also depends on the fractional order α. Namely, rewriting relation (7) in integral form

$$\int_0^t dt=\int_{x_{\max}}^{x}\frac{dx}{x\sqrt{1-\dfrac{2}{\alpha+1}|x|^{\alpha-1}}}, \tag{13}$$

and evaluating (13) for $x(\dot{x}_{\max})=1$ the following time period is obtained:

$$T_1=\ln\frac{\sqrt{\dfrac{2}{\alpha+1}}}{1+\sqrt{1-\dfrac{2}{\alpha+1}}}=\ln\left(\sqrt{\frac{\alpha+1}{2}}+\sqrt{\frac{\alpha-1}{2}}\right). \tag{14}$$

In Table 2 the time period T_1 for various values of α is given.

Analyzing (14) and the values given in Table 2, it can be concluded that the higher the value of α the time period T_1 is longer. Besides, from (13) is evident that independently of α, the time necessary for homoclinic orbit to reach the saddle point, i.e., $x\to0$, is infinitely long, i.e., $t\to\infty$. The same result is given by Guckenheimer and Holmes [2] for the cubic nonlinearity.

Table 1

α	4/3	3/2	5/3	2	3
$x_{\max}$	1.5880	1.5625	1.5396	1.5000	1.4142
$\dot{x}_{\max}$	0.37796	0.44721	0.50000	0.57735	0.70711

Table 2

α	4/3	3/2	5/3	2	3
T_1	0.39768	0.48121	0.54931	0.65848	0.88137

The homoclinic orbit separates the phase plane into two areas. Inside the separatrix curve the orbits are around one of the centers, and outside the separatrix curve the orbits surround both the centers and the saddle point. Physically it means that for certain initial conditions the oscillations are around one steady-state position, and for others around all the steady-state solutions (two stable and an unstable).

2.1. Melnikov's criteria for chaos

Let us form Melnikov's function for (1) and $\Gamma_+^0(t)$, i.e. $\Gamma_-^0(t)$ given by (8) and (9)

$$M(t_0)=\int_{-\infty}^{+\infty}\dot{x}^0(t)[\gamma\cos\omega(t+t_0)-\delta\dot{x}^0(t)]\,dt, \tag{15}$$

where

$$\dot{x}^0(t)=-\sqrt[\alpha-1]{\frac{\alpha+1}{2}}\left[\operatorname{sech}\left(\frac{\alpha-1}{2}t\right)\right]^{2/(\alpha-1)}\tanh\left(\frac{\alpha-1}{2}t\right),$$

$$x^0=\sqrt[\alpha-1]{\frac{\alpha+1}{2}}\left[\operatorname{sech}\left(\frac{\alpha-1}{2}t\right)\right]^{2/(\alpha-1)}. \tag{16}$$

Substituting (16) into (15) the transformed Melnikov's function is obtained

$$\begin{aligned}M(t_0)=&-\gamma\left(\frac{\alpha+1}{2}\right)^{1/(\alpha-1)}\int_{-\infty}^{+\infty}\left[\operatorname{sech}\left(\frac{\alpha-1}{2}t\right)\right]^{2/(\alpha-1)}\tanh\left(\frac{\alpha-1}{2}t\right)\cos\omega(t+t_0)\,dt\\&-\delta\left(\frac{\alpha+1}{2}\right)^{2/(\alpha-1)}\int_{-\infty}^{+\infty}\left[\operatorname{sech}\left(\frac{\alpha-1}{2}t\right)\right]^{4/(\alpha-1)}\left[\tanh\left(\frac{\alpha-1}{2}t\right)\right]^2dt,\end{aligned} \tag{17}$$

i.e.,

$$M(t_0)=-\gamma\left(\frac{\alpha+1}{2}\right)^{1/(\alpha-1)}\cos\omega t_0 I_1+\gamma\left(\frac{\alpha+1}{2}\right)^{1/(\alpha-1)}\sin\omega t_0 I_2-\delta\left(\frac{\alpha+1}{2}\right)^{2/(\alpha-1)}I_3, \tag{18}$$

where

$$I_1=\int_{-\infty}^{+\infty}\frac{\sinh\left(\frac{\alpha-1}{2}t\right)}{\left[\cosh\left(\frac{\alpha-1}{2}t\right)\right]^{(\alpha+1)/(\alpha-1)}}\cos\omega t\,dt, \tag{19}$$

$$I_2=\int_{-\infty}^{+\infty}\frac{\sinh\left(\frac{\alpha-1}{2}t\right)}{\left[\cosh\left(\frac{\alpha-1}{2}t\right)\right]^{(\alpha+1)/(\alpha-1)}}\sin\omega t\,dt, \tag{20}$$

$$I_3=\int_{-\infty}^{+\infty}\frac{\left[\sinh\left(\frac{\alpha-1}{2}t\right)\right]^2}{\left[\cosh\left(\frac{\alpha-1}{2}t\right)\right]^{2(\alpha+1)/(\alpha-1)}}\,dt. \tag{21}$$

The first integral I_1 in (19) is zero, since it is the product of an odd and an even function.

Integral I_2: Using the partial integration the integral I_2 is transformed into the following form:

$$I_2 = 2\int_0^{+\infty} \frac{\sinh\left(\frac{\alpha-1}{2}t\right)}{\left[\cosh\left(\frac{\alpha-1}{2}t\right)\right]^{(\alpha+1)/(\alpha-1)}} \sin\omega t\, dt = \frac{4}{\alpha-1}\int_0^{+\infty} \frac{\sinh(x)}{[\cosh(x)]^{(\alpha+1)/(\alpha-1)}} \sin\left(\frac{2\omega x}{\alpha-1}\right) dx$$
$$= -2\left[\frac{\sin\left(\frac{2\omega x}{\alpha-1}\right)}{[\cosh(x)]^{2/(\alpha-1)}}\right]_0^{\infty} + \frac{4\omega}{\alpha-1}\int_0^{+\infty} \frac{\cos\left(\frac{2\omega x}{\alpha-1}\right)}{[\cosh(x)]^{2/(\alpha-1)}}\, dx. \tag{22}$$

The first term in the integral is zero and the second has the exact analytical solution for $\alpha>1$ (see [51])

$$I_2 = \frac{\omega}{\alpha-1}\frac{2^{2/(\alpha-1)}}{\Gamma\left(\frac{2}{\alpha-1}\right)}\Gamma\left(\frac{1+i\omega}{\alpha-1}\right)\Gamma\left(\frac{1-i\omega}{\alpha-1}\right), \tag{23}$$

where Γ is the Euler gamma function and $i=\sqrt{-1}$ is the imaginary unit.

Special cases:

1. For $\alpha=3$, when $\Gamma(1)=1$ and $|\Gamma(1/2+i\omega/2)|^2=\pi/\cosh(\pi\omega/2)$, (see [51]), the value of the integral is

$$I_2(\alpha=3) = \omega\pi\,\mathrm{sech}\left(\frac{\pi\omega}{2}\right). \tag{24}$$

The result is equal to that obtained by the use of the method of residues (see [2]).

2. For $\alpha=2$ when $\Gamma(1+i\omega)\Gamma(1-i\omega)=\pi\omega/\sinh(\pi\omega)$ and $\Gamma(2)=1$ (see [51])

$$I_2 = \frac{4\pi\omega^2}{\sinh(\pi\omega)}. \tag{25}$$

3. If $2/(\alpha-1)$ in (22) is an even integer number, i.e., $2/(\alpha-1)=2n$, $n\geqslant 2$, the exact analytical solution for the integral I_2 is given by Gradstein and Rjizhik [51]

$$I_2 = \frac{4^n\pi n^2\omega^2}{(2n-1)!\sinh(n\pi\omega)}\prod_{k=1}^{n-1}(\omega^2n^2+k^2). \tag{26}$$

4. If $2/(\alpha-1)$ is an odd integer number, i.e., $2/(\alpha-1)=2n+1$, $n\geqslant 1$, the analytical expression of the integral I_2 is

$$I_2 = \frac{2^{2n}(2n+1)\pi\omega}{(2n)!\cosh\left(\frac{\pi\omega(2n+1)}{2}\right)}\prod_{k=1}^{n}\left[\frac{\omega^2(2n+1)^2}{4}+\left(\frac{2k-1}{2}\right)^2\right]. \tag{27}$$

Integral I_3: After partial integration and using the boundary conditions, the integral I_3 simplifies to

$$I_3 = \frac{2(\alpha-1)}{\alpha+3}\int_0^{+\infty} \frac{dt}{\left[\cosh\left(\frac{\alpha-1}{2}t\right)\right]^{4/(\alpha-1)}} = \frac{4}{\alpha+3}\int_0^{+\infty}\frac{dx}{\cosh^{4/(\alpha-1)}(x)}. \tag{28}$$

Unfortunately, the integral (28) has not a closed form analytical solution for all values of $\alpha>1$. Some special cases are considered:

1. For $4/(\alpha-1)=2n$, where $(2n)$ is a whole even number and $n\geqslant 2$, the solution of (28) is

$$I_3 = \frac{(2n)}{(2n)^2-1}\frac{2^{n-1}(n-1)!}{(2n-3)!!}, \tag{29}$$

where

$$(n-1)! = 1,2,\ldots,(n-1), \quad (2n-3)!! = 1,3,\ldots,(2n-3).$$

According to (29), for the special case when $\alpha=3$, i.e., $(2n)=2$, we obtain $I_3=\frac{2}{3}$. This result corresponds to the value given in Guckenheimer and Holmes [2].

2. If $4/(\alpha-1)$ is an odd number, i.e., $4/(\alpha-1)=(2n+1)$, where $n\geqslant 1$, the evaluation of the integral gives

$$I_3 = \frac{\pi(2n+1)(2n-1)!!}{4(n+1)(2n)!!}, \tag{30}$$

where $(2n)!! = 2,4,6,\ldots,(2n+1)!! = 1,3,5,\ldots$.

Table 3

α	I_2	I_3	$\left(\frac{\gamma}{\delta}\right)_c$	$\left(\frac{\gamma}{\delta}\right)_c$, $\omega=1$
4/3	$\frac{24\pi\omega^2(1+9\omega^2)(4+9\omega^2)}{5\sinh(3\pi\omega)}$	0.34099	$\frac{0.11281\sinh(3\pi\omega)}{\pi\omega^2(1+9\omega^2)(4+9\omega^2)}$	1.7114
7/5	$\frac{5\pi\omega(1+25\omega^2)(9+25\omega^2)}{24\cosh\left(\frac{5\pi\omega}{2}\right)}$	0.36941	$\frac{2.7971\cosh\left(\frac{5\pi\omega}{2}\right)}{\pi\omega(1+25\omega^2)(9+25\omega^2)}$	1.2972
3/2	$\frac{32\pi\omega^2(4\omega^2+1)}{3\sinh(2\pi\omega)}$	0.40635	$\frac{5.9524\times10^{-2}\sinh(2\pi\omega)}{\pi\omega^2(4\omega^2+1)}$	1.0146
5/3	$\frac{3\pi\omega(1+9\omega^2)}{2\cosh\left(\frac{3\pi\omega}{2}\right)}$	0.45714	$\frac{0.46921\cosh\left(\frac{3\pi\omega}{2}\right)}{\pi\omega(1+9\omega^2)}$	0.83135
2	$\frac{4\pi\omega^2}{\sinh(\pi\omega)}$	0.53333	$\frac{0.2\sinh(\pi\omega)}{\pi\omega^2}$	0.73521
3	$\frac{\pi\omega}{\cosh\left(\frac{\pi\omega}{2}\right)}$	0.66667	$\frac{0.94281\cosh\left(\frac{\pi\omega}{2}\right)}{\pi\omega}$	0.75302

Using the previous results and Melnikov's theorem [21] the following is stated:

Proposition: *If $M(t_0)$ has a simple zero and the corresponding critical parameter value is*

$$\left(\frac{\gamma}{\delta}\right)_{cr}=\left(\frac{\alpha+1}{2}\right)^{1/(\alpha-1)}\frac{I_3}{I_2}, \tag{31}$$

then in the system with fractional order displacement (1) the deterministic chaos may appear for certain parameter values which satisfy the relation

$$\frac{\gamma}{\delta}>\left(\frac{\gamma}{\delta}\right)_{cr}. \tag{32}$$

Remark. For (31) the distance between the stable and unstable manifolds of the homoclinic point $(0,0)$ is zero and the manifolds intersect transversely forming the transverse homoclinic orbits. The presence of such orbits implies that for certain parameters (32) the Poincare map of the system with fractional order displacement (1) has the strange attractor and the countable infinity of unstable periodic orbits, an uncountable set of bounded non-periodic orbits and a dense orbit which are the main characteristics of the chaotic motion.

Relation (32) with (31) represents the analytical criteria for chaos.

In Table 3 the critical parameters for various fraction values α, and specially when $\omega=1$, are shown.

Analyzing the critical parameter $(\gamma/\delta)_c$ in Table 3 it can be concluded that it increases by decreasing the parameter α.

3. Numerical simulation

Let us consider the set of three first-order differential equations

$$\dot{x}=y,\quad \dot{y}-x+x|x|^{\alpha-1}=\varepsilon(\gamma\cos\omega t-\delta y),\quad \dot{t}=1. \tag{33}$$

For $\omega=1$ and

$$\frac{(\gamma/\delta)}{(\gamma/\delta)_c}=k, \tag{34}$$

the system of differential equations (33) is rewritten as

$$\dot{x}=y,\quad \dot{y}-x+x|x|^{\alpha-1}=\varepsilon\left(k\delta\left(\frac{\gamma}{\delta}\right)_c\cos t-\delta y\right),\quad \dot{t}=1, \tag{35}$$

where according to (31) the critical parameter value $(\gamma/\delta)_c$ depends on α.

To prove the accuracy of the analytical solving procedure, the numerical simulation is done. The phase plane diagrams and Poincare maps are plotted for certain values of α. The parameter k is varied and δ is assumed as a fixed constant. Three examples are investigated.

1. For $\alpha=2$ and $\varepsilon\delta=0.3$ the differential equation of motion has the form

$$\ddot{x}+0.3\dot{x}-x+x|x|=0.220563k\cos t, \tag{36}$$

where the critical parameter value is $(\gamma/\delta)_c=0.7351$ (see Table 3). In Fig. 1 the phase diagrams and the Poincare maps for $k=0.9$ and 3.5 and also $k=3$ for initial conditions $x(0)=1$ and $\dot{x}(0)=0$ are plotted. The orbits in Fig. 1a are periodical with period $1T$. In Fig. 1b the phase diagram corresponds to chaotic motion and the Poincare map forms the strange attractor.

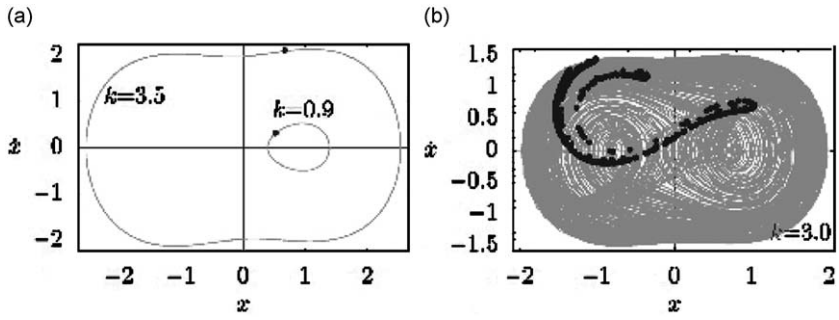

Fig. 1. Phase plane diagram and Poincare map for $\alpha = 2$ and $\delta = 0.3$: (a) $k = 0.9$ and 3.5, (b) $k = 3$.

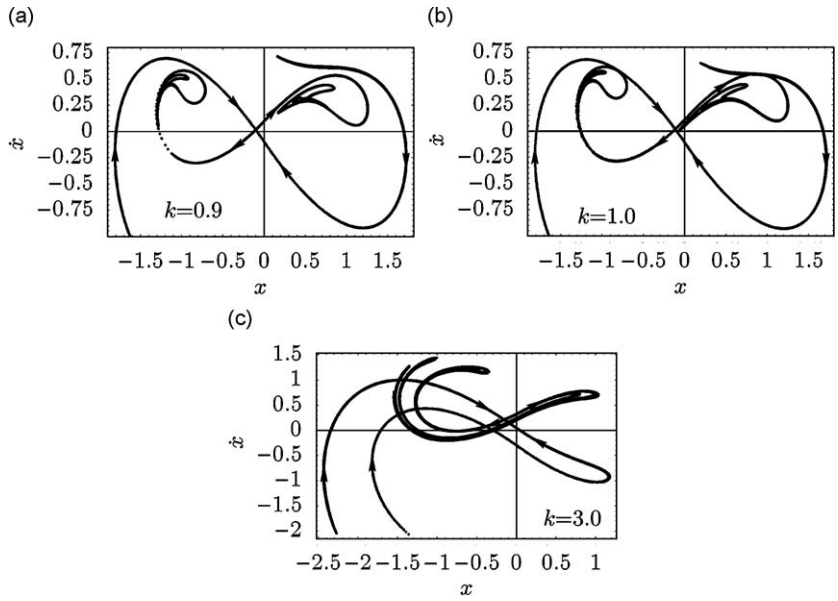

Fig. 2. Poincare maps for the Duffing equation, showing stable and unstable manifolds of the saddle point near (0,0) for $\alpha = 2$, $\varepsilon\delta = 0.3$: (a) $k = 0.9$, (b) $k = 1$ and (c) $k = 3$.

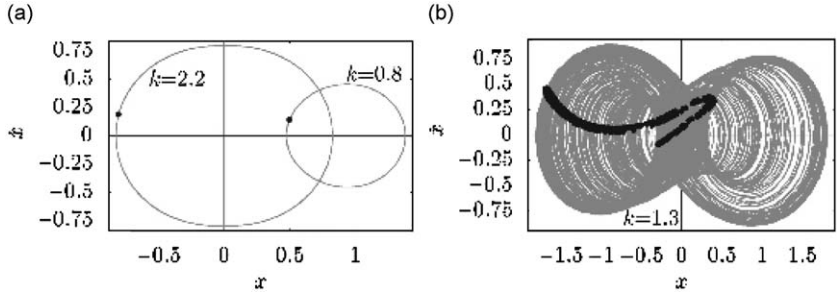

Fig. 3. Phase plane diagram and Poincare map for $\alpha = \frac{4}{3}$ and $\varepsilon\delta = 0.25$: (a) $k = 0.8$ and 2.2; (b) $k = 1.3$.

In Fig. 2 the Poincare maps for (36), showing stable and unstable manifolds of the saddle point near (0,0) for $k = 0.9, 1$ and 3 are plotted. These are computed numerically. It can be seen that the first tangency appears to occur about $k = 1$, the value which according to (34) corresponds to the theoretically obtained value $(\gamma/\delta)_c = 0.7351$.

2. For the fractional order $\alpha = \frac{4}{3}$ and parameter values: $\varepsilon\delta = 0.25$ and $(\gamma/\delta)_c = 1.7114$ (see Table 3), the differential equation of motion is

$$\ddot{x} + 0.25\dot{x} - x + x|x|^{1/3} = 0.42785k\cos t. \tag{37}$$

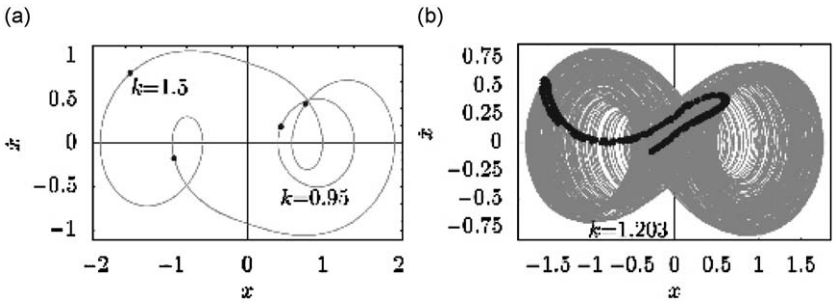

Fig. 4. Phase plane diagram and Poincare map for $\alpha=\frac{7}{5}$ and $\varepsilon\delta=0.3$: (a) $k=0.95$ and 1.5; (b) $k=1.203$.

In Fig. 3 the phase plane diagrams and the Poincare maps are plotted. For $k=0.8$ and 2.2 the motion is periodical (see Fig. 3a) and for $k=1.3$ chaotic (see Fig. 3b).

3. If the fractional order is $\alpha=\frac{7}{5}$, the critical parameter $(\gamma/\delta)_c=1.2972$ and $\varepsilon\delta=0.3$, the following differential equation exists:

$$\ddot{x}+0.3\dot{x}-x+x|x|^{2/5}x=0.38916k\cos t. \tag{38}$$

In Fig. 4 the phase plane diagrams and the Poincare maps are plotted for $k=0.95$, 1.5 and 1.203. It is obvious that for $k=0.95$ and 1.5 the motion is $1T$ and $3T$ periodical, respectively (Fig. 4a). For $k=1.203$ the motion is chaotic (see Fig. 4b) and the strange attractor is evident.

From the previous consideration it can be concluded that chaotic motion appears for $k>1$. Comparing this result of numerical simulation with the analytically obtained one (32), we see that they agree. For $k>1$ the motion may be steady-state chaotic.

4. The Lyapunov exponents and bifurcation diagrams

The chaotic motion of dynamic systems is usually studied numerically through the concept of Lyapunov characteristic exponents and bifurcation diagrams. Both approaches are applied for the dynamic system (35).

Lyapunov exponents quantify the chaotic behavior of the system. For the dynamic system (35) the Lyapunov spectrum is computed using Mathematica, as it is suggested by Sandri [52]. Varying the value of k the bifurcation $x-k$ diagram is obtained.

In Figs. 4–6 the bifurcation diagrams and the Lyapunov spectrums for (36)–(38) are plotted. Analyzing the diagrams the following is concluded:

1. As the topological dimension of system (35) is three, the chaotic motion appears for the case when one of the Lyapunov exponents is positive. For this nonautonomous model there is a spurious Lyapunov exponent which converges to zero. It corresponds to the additional trivial evolution equations $\dot{t}=1$. The third Lyapunov exponent is negative.
2. The Lyapunov spectrum and the bifurcation diagram are in good agreement. Namely, the intervals of chaotic motion plotted in bifurcation diagrams correspond to those where one of the Lyapunov exponents is positive.
3. The chaos is the result of the period doubling bifurcation and is manifested for $k>0$.
4. In Figs. 5–7 the widening of the chaotic attractor is visible.
5. For $\alpha=2$ and $k\in[1.3,1.55]\wedge[2.1,2.4]\wedge[2.65,3.4]$ one of the Lyapunov exponents is positive and the bifurcation diagram shows the chaos. The same correlation is seen for $\alpha=\frac{4}{3}$ and $k\in[1.1,1.58]$ and also for $\alpha=\frac{7}{5}$ and $k\in[1.05,1.39]$.
6. For all of the three examples it is evident that the motion is not chaotic for $k<1$, i.e., for $(\gamma/\delta)<0.7351$ when $\alpha=2$, $(\gamma/\delta)<(\gamma/\delta)_c=1.7114$ when $\alpha=\frac{4}{3}$ and $(\gamma/\delta)<(\gamma/\delta)_c=1.2972$ for $\alpha=\frac{7}{5}$. The obtained values are in good agreement with analytical results obtained by using Melnikov's criteria and with numerical simulations.

5. Control of chaos

The delayed feedback control, i.e., the 'Pyragas method' [32] is based on the idea of the stabilization of unstable periodic orbits embedded within a strange attractor. This is achieved by making a small time-dependent perturbation in the form of feedback to an accessible system parameter. The method turns the presence of chaos into an advantage. Due to the infinite number of different unstable periodic orbits embedded in a strange attractor, a chaotic system can be tuned to a large number of distinct periodic regimes by watching the temporal programming of small parameter perturbation to stabilize different periodic orbits.

The introduced simple control law in Pyragas [27] is

$$F(t)=K[\dot{x}(t-\tau)-\dot{x}(t)], \tag{39}$$

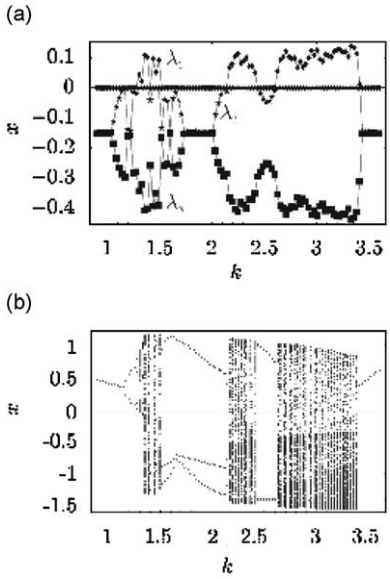

Fig. 5. The Lyapunov's spectra (a) and bifurcation diagram (b) for $\alpha = 2$.

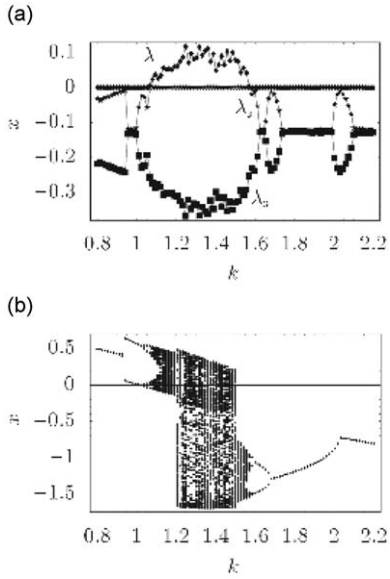

Fig. 6. The Lyapunov's spectra (a) and bifurcation diagram (b) for $\alpha = \frac{4}{3}$.

where K is a constant called the weight of perturbation and τ is the time-delay. The system with the controlling function is

$$\ddot{x} + \delta\dot{x} - x + x|x|^{\alpha-1} = \gamma\cos(\omega t) + K[\dot{x}(t-\tau) - \dot{x}(t)]. \tag{40}$$

The control procedure depends on the parameters K and τ. As the system is T-periodic and the goal is to stabilize a forced T-periodic solution, we choose $\tau = T$. The weight K of the feedback is adjusted by numerical experiment.

The control procedure is applied to the three examples mentioned in the previous section. For $\alpha = 2$, $\delta = 0.3$, $k = 3$ the chaotic motion is transformed into a periodical one when the control parameter is $K = 0.5$ and the time delay $\tau = \pi$ (Fig. 8). The chaos control is achieved with the weight of perturbation $K = 0.5$ and the time delay $\tau = 2\pi$ in the system where $\alpha = \frac{4}{3}$, $\delta = 0.25$, $k = 1.3$ (Fig. 9), and also $\alpha = \frac{7}{5}$, $\delta = 0.3$, $k = 1.203$ (Fig. 10).

The numerical experiment shows that the control procedure is seriously sensitive to the value of parameter K. In Fig. 11, the x–K diagram for $\alpha = 2$, $\delta = 0.3$, $k = 3$ is plotted. It is evident that choosing an appropriate weight K of the feedback the stabilization is achieved, the unstable periodic orbit becomes stable and the chaotic motion is transformed into periodical one.

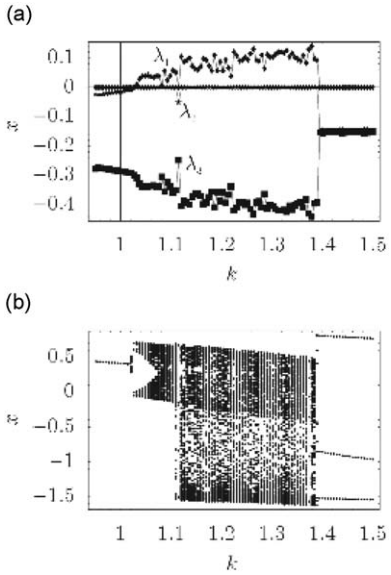

Fig. 7. The Lyapunov's spectra (a) and bifurcation diagram (b) for $\alpha = \frac{7}{5}$.

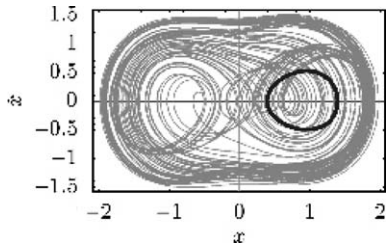

Fig. 8. The phase plane diagrams for $\alpha = 2$, $\varepsilon\delta = 0.3$ and $k = 3$ before (grey curve) and after chaos control (black curve).

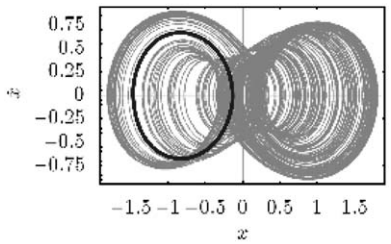

Fig. 9. The phase plane diagrams for $\alpha = \frac{4}{3}$, $\varepsilon\delta = 0.25$ and $k = 1.3$ before (grey curve) and after chaos control (black curve).

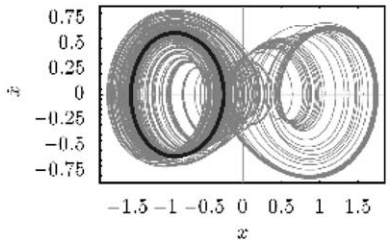

Fig. 10. The phase plane diagrams for $\alpha = \frac{7}{5}$, $\varepsilon\delta = 0.3$ and $k = 1.203$ before (grey curve) and after chaos control (black curve).

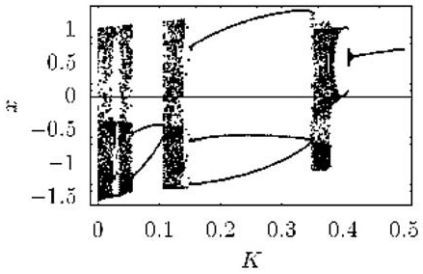

Fig. 11. The $x-K$ diagram for $\alpha = 2$, $\varepsilon\delta = 0.3$, $k = 3$.

6. Conclusion

The following can be concluded:

1. In dynamical systems with fractional order displacement, and small damping and excitation, and where the homoclinic orbit exists, it is shown that chaos may appear.
2. For the system with fractional order displacement the exact analytical formulation of the homoclinic orbit is obtained. The homoclinic orbit strongly depends on the fractional order α. The homoclinic orbit of the cubic Duffing oscillator is one special case and can be obtained from the general analysis given.
3. Melnikov's procedure adopted for systems with fractional order displacement gives analytical criteria for chaos depending on the relationship between the (δ/γ) and the critical $(\delta/\gamma)_c$ parameter value. The exact analytical critical parameter values $(\delta/\gamma)_c$ can be obtained dependently on fractional order α.
4. The numerical simulation shows the dependence of the motion type (periodic and chaotic) on the variation of parameter values. The phase plane diagrams and the Poincare maps for certain parameter values give the results which were expected according to the analytical procedure.
5. The Lyapunov exponents and the bifurcation diagrams show the period-doubling bifurcation and the transformation from periodic to chaotic motion and vice versa. The results obtained show the correctness of the analysis.
6. In systems with fractional order displacement chaos control by means of delayed self-controlling feedback is investigated, and motion is transformed from chaos to periodicity.

Acknowledgment

This investigation is supported by the Ministry of Science, Republic of Serbia (Proj. no. 144008).

References

[1] L. Cveticanin, Oscillator with fraction order restoring force, *Journal of Sound and Vibration* 320 (2008) 1064–1077.
[2] J. Guckenheimer, P. Holmes, *Nonlinear Oscillations, Dynamical Systems, and Bifurcations of Vector Fields*, Springer, New York, 1983.
[3] S. Wiggins, *Global Bifurcations and Chaos: Analytical Methods*, Springer, New York, 1988.
[4] W.Y. Tseng, J. Dugundji, Nonlinear vibrations of a buckled beam under harmonic excitation, *Journal of Applied Mechanics* 38 (1971) 467–476.
[5] P. Holmes, A nonlinear oscillator with a strange attractor, *Philosophical Transactions of the Royal Society of London Series A* 292 (1979) 419–448.
[6] P. Holmes, J. Marsden, A partial differential equation with infinitely many periodic orbits: chaotic oscillations of a forced beam, *Archives for Rational Mechanics and Analysis* 76 (1981) 135–166.
[7] G. Prathap, T.K. Varadan, The inelastic large deformation of beams, *Journal of Applied Mechanics* 43 (1976) 689–690.
[8] C.C. Lo, S.D. Gupta, Bending of a nonlinear rectangular beam in large deflection, *Journal of Applied Mechanics* 45 (1978) 213–215.
[9] G. Lewis, F. Monasa, Large deflections of cantilever beams of non-linear material of the Ludwick type subjected to an end moment, *International Journal of Non-Linear Mechanics* 17 (1982) 1–6.
[10] H.W. Haslach, Post-buckling behavior of columns with non-linear constitutive equations, *International Journal of Non-Linear Mechanics* 20 (1982) 53–67.
[11] H.W. Haslach, Influence of adsorbed moisture on the elastic post-buckling behavior of columns made of non-linear hydrophilic polymers, *International Journal of Non-Linear Mechanics* 27 (1992) 527–546.
[12] W-H. Chen, R.F. Gibson, Property distribution for nonuniform composite beams from vibration response measurements and Galerkin's method, *Journal of Applied Mechanics* 65 (1988) 127–133.
[13] G. Duffing, *Erzwungene Schwingungen bei veranderlicher Eigenfrequenz und ihre technische Bedeutung, Druck und Verlag vor Friedr*, Vieweg & Sohn, Braunschweig, 1918.
[14] D. Russell, T. Rossing, Testing the nonlinearity of piano hammers using residual shock spectra, *Acustica—Acta Acustica* 84 (1998) 967–975.
[15] Q. Zhu, M. Ishitoby, Chaos and bifurcations in a nonlinear vehicle model, *Journal of Sound and Vibration* 275 (2004) 1136–1146.
[16] W.N. Patten, S. Sha, C. Mo, A vibration model of open celled polyurethane foam automative seat cushions, *Journal of Sound and Vibration* 217 (1998) 145–161.
[17] C.V. Jutte, Generalized Synthesis Methodology of Nonlinear Springs for Prescribed Load—Displacement Functions, PhD Dissertation, Mechanical Engineering, The University of Michigan, 2008.
[18] J.F. Rhoads, Generalized parametric resonance in electrostatically actuated micromechanical oscillators, *Journal of Sound and Vibration* 296 (2006) 797–829.
[19] J.F. Rhoads, Tunable micromechanical filters that exploit parametric resonance, *Journal of Vibration and Acoustics* 127 (2005) 423–430.

[20] C. Cortopassi, O. Englander, *Nonlinear Springs for Increasing the Maximum Stable Deflection of MEMS Electrostatic Gap Closing Actuators*, UC Berkeley, ⟨http://robotics.eecs.berkeley.edu/~pister/245/project/CortopassiEnglander⟩, March 10, 2009.
[21] V.K. Melnikov, On the stability of the center for time periodic perturbations, *Transactions of the Moscow Mathematical Society* 12 (1963) 1–57.
[22] P. Holmes, A nonlinear oscillator with a strange attractor, *Philosophical Transactions of the Royal Society of London, Series A, Mathematical and Physical Sciences* 292 (1979) 419–448.
[23] R. Chacon, General result on chaos suppression for biharmonically driven dissipative systems, *Physics Letters A* 257 (1999) 293–300.
[24] L. Cveticanin, Extension of Melnikov criterion for the differential equation with complex function, *Nonlinear Dynamics* 4 (1993) 139–152.
[25] R. Wang, J. Deng, Z. Jing, Chaos, control in Duffing system, *Chaos, Solitons and Fractals* 23 (2006) 249–257.
[26] J. Yang, Z. Jing, Control of chaos in a three-well duffing system, *Chaos, Solitons and Fractals*, in press (doi:10.1016/j.chaos.2008.05018).
[27] K. Pyragas, Continuous control of chaos by self controlling feedback, *Physics Letters A* 170 (1992) 421–428.
[28] K. Pyragas, Continuous control of chaos by self-controlling feedback, *Controlling Chaos*, Academic Press, San Diego, 1996, pp. 118–123.
[29] T. Ushio, Limitation of delayed feedback control in nonlinear discrete-time systems, *IEEE Transactions on Circuits and Systems I* 43 (1996) 815–816.
[30] G.R. Chen, X.H. Yu, On time-delayed feedback control of chaotic systems, *IEEE Transactions on Circuits and Systems I* 46 (1999) 767–772.
[31] K. Pyragas, Control of chaos via an unstable delayed feedback controller, *Physical Review Letters* 86 (2001) 2265–2268.
[32] K. Pyragas, Delayed feedback control of chaos, *Philosophical Transactions of the Royal Society A: Mathematical, Physical and Engineering Sciences* 364 (2006) 2309–2334.
[33] J. Zhu, Y.-P. Tian, Necessary and sufficient conditions for stabilizability of discrete-time systems via delayed feedback control, *Physics Letters A* 343 (2005) 95–107.
[34] E.N. Dudnik, Yu.I. Kuznetsov, I.I. Minakova, Yu.M. Romanovskiii, Synchronization in systems with strange attractors, *Moscow University Physics Bulletin Series* 3 (24) (1983) 84–87.
[35] R. Chacon, Maintenance and suppression of chaos by weak harmonic perturbations: a unified view, *Physical Review Letters* 86 (2001) 1737–1740.
[36] R. Lima, M. Pettini, Suppression of chaos by resonant parametric perturbations, *Physical Review A* 41 (1990) 726–733.
[37] R. Lima, M. Pettini, Parametric resonant control of chaos, *International Journal of Bifurcation and Chaos* 8 (1998) 1675–1684.
[38] A.Y. Zhalnin, Control of chaos in nonautonomous systems with quasiperiodic excitation, *Technical Physics Letters* 25 (1999) 662–664.
[39] K.A. Mirus, J.C. Sprott, 1999, Controlling chaos in low-and high-dimensional systems with periodic parametric perturbations, *Physical Review E* 59 (1999) 5313–5324.
[40] M. Belhaque, M. Houssni, Quasi-periodic oscillations, chaos and suppression of chaos in a nonlinear oscillator driven by parametric and external excitations, *Nonlinear Dynamics* 18 (1999) 1–24.
[41] A.N. Pisarchik, R. Corbalan, Parametric nonfeedback resonance in period doubling systems, *Physical Review E* 59 (1999) 1669–1674.
[42] J. Yang, Z. Jing, Inhibition of chaos in a pendulum equation, *Chaos, Solitons and Fractals* 33 (2008) 726–737.
[43] K. Pyragas, F. Lange, T. Letz, J. Parisi, A. Kittel, Stabilization of an unstable steady state in intracavity frequency-doubled lasers, *Physical Review E—Statistical Physicas, Plasmas, Fluids, and Related Interdisciplinary Topics* 61 (4A) (2000) 3721–3731.
[44] K. Pyragas, F. Lange, T. Letz, J. Parisi, A. Kittel, Dynamics and control of a multimode laser: reduction of space-dependent rate equations to a low dimensional system, *Physical Review E—Statistical, Nonlinear and Soft Matter Physics* 63 (2001) 1–12.
[45] W.H. Hai, Y.W. Duan, L.X. Pan, An analytical study for controlling unstable periodic motion in magneto-elastic chaos, *Physics Letters A* 234 (1997) 198–204.
[46] T. Hikihara, M. Touno, T. Kawagoshi, Experimental stabilization of unstable periodic orbit in magneto-elastic chaos by delayed feedback control, *International Journal of Bifurcation and Chaos* 7 (1997) 2837–2846.
[47] A.L. Fradkov, R.J. Evans, B.R. Andrievsky, Control of chaos: methods and applications in mechanics, *Philosophical Transactions of the Royal Society A* 364 (2006) 2279–2307.
[48] V. Pyragas, K. Pyragas, Delayed feedback control of the Lorenz system: an analytical treatment at a subcritical Hopf bifurcation, *Physical Review E—Statistical, Nonlinear and Soft Matter Physics* 73 (036215) (2006) 1–10.
[49] M. Zukovic, L. Cveticanin, Chaotic response in a stable Duffing system of non-ideal type, *Journal of Vibration and Control* 13 (2007) 751–767.
[50] M. Zukovic, L. Cveticanin, Chaos in non-ideal mechanical system with clearance, *Journal of Vibration and Control* (2009) (doi:10.1177/1075546308091216).
[51] I.S. Gradstein, I.M. Rjizhik, *Tablici integralov, summ, rjadov i proizvedenij*, Nauka, Moscow, 1971.
[52] M. Sandri, Numerical calculation of Lyapunov exponents, *The Mathematical Journal* 6 (1996) 78–84.